COMPUTATIONS OF HEEGAARD FLOER HOMOLOGY GROUPS

ANDRÁS I. STIPSICZ

Abstract. After reviewing basic concepts and constructions of (the hat-version of) Heegaard Floer homology groups of closed 3–manifolds, we show a way to compute these groups in associated (extended) grid diagrams.

MSC 2010. 57R58.

Key words. Heegaard diagrams, Heegaard Floer homology, branched covers, grid diagrams

1. INTRODUCTION

Heegaard Floer invariants of 3– and 4–manifolds, knots in 3–manifolds and contact structures on 3–manifolds have played central role in the resolutions of many important problems of low dimensional topology. In the present note we focus on the developement of computations of (the hat version of) Heegaard Floer homology groups $\widehat{\mathrm{HF}}$ of closed oriented 3–manifolds. These invariants (among further versions of the theory, not discussed in these notes) were introduced by Peter Ozsváth and Zoltán Szabó in their seminal paper [7]. The definition of the invariants rests on simple 3–dimensional notions (most notably on the theory of Heegaard decompositions and diagrams), and fairly advanced techniques of symplectic topology (the concept of Lagrangian Floer homology). While the 3–dimensional background is rather combinatorial, Lagrangian Floer homology theory requires the study of moduli spaces of holomorphic maps from the unit disk into high dimensional symplectic (and therefore almost-complex) manifolds. The study of such moduli spaces, resting on Gromov's seminal paper [2] and infinite dimensional global analysis, leads to intricate complex geometry. In addition, the nature of the definition of these moduli spaces (as solutions of a partial differential equation provided by the $\overline{\partial}$–operator) makes direct and explicit computations rather difficult. Despite this complexity, beautiful and deep results were achieved by the use of Heegaard Floer invariants.

In 2006 the work of Sarkar and Wang [10] provided a breakthrough in the computational aspects of the theory: in their aforementioned paper it has been shown that for specific Heegaard diagrams the Heegaard Floer group $\widehat{\mathrm{HF}}(Y)$ of a closed, oriented 3–manifold Y can be computed in a purely combinatorial

manner. Diagrams with similar properties were found in [5], and in [6] it has been shown that (the appropriate stable version of) the hat-version of Heegaard Floer homology is a purely combinatorial theory.

After a brief review of the 3–dimensional and the symplectic topological background in Section 2, we give the definition of the hat-version of Heegaard Floer homology groups in Section 3. Nice diagrams will be discussed in Section 4, and finally we give a simple computational scheme (resting on the branched cover construction) for the homologies in Section 5.

2. BACKGROUND

2.1. Heegaard decompositions and diagrams of 3–manifolds. Suppose that Y is a closed, oriented, smooth 3–dimensional manifold. It is a standard fact (and follows, for example, from the existence of a Morse function, or a triangulation on Y) that Y admits a *Heegaard decomposition* $\mathfrak{U} = (U_0, U_1, \Sigma)$, i.e.,

$$Y = U_0 \cup_\Sigma U_1,$$

where U_0, U_1 are genus-g handlebodies and $\Sigma = \partial U_0 = -\partial U_1$ is a genus-g surface (the *Heegaard surface* of the decomposition). This simply means that Y can be given by gluing two genus-g handlebodies together along their (diffeomorphic) boundaries. For example, the 3–sphere S^3 can be decomposed as the union of two disks, giving a genus-0 Heegaard decomposition $\mathfrak{S}$, and also as the union of the solid unknotted torus and its complement, providing the standard toric Heegaard decomposition $\mathfrak{T}$ of S^3. By taking the connected sum point on the Heegaard surfaces Σ_i, the Heegaard decompositions $\mathfrak{U}_i = (U_0^i, U_1^i, \Sigma_i)$ of Y_i ($i = 1, 2$) provide a Heegaard decomposition $\mathfrak{U} = (U_0^1 \natural U_0^2, U_1^1 \natural U_1^2, \Sigma_1 \# \Sigma_2)$ of the connected sum $Y = Y_1 \# Y_2$. The connected sum of a Heegaard decomposition $\mathfrak{U}$ with the standard toric decomposition $\mathfrak{T}$ of S^3 is called the *stabilization* of $\mathfrak{U}$. The following theorem is of fundamental importance in our discussions.

THEOREM 2.1 (Reidemeister, Singer [9, 11]). *Two Heegaard decompositions $\mathfrak{U}_1$ and $\mathfrak{U}_2$ of the same 3–manifold Y admit common stabilization.*

Next we would like to give a simple presentation of a genus-g handlebody $\mathfrak{U}$. To this end, suppose that $\boldsymbol{\alpha} = \{\alpha_1, \ldots, \alpha_k\}$ is a collection of disjoint, embedded simple closed curves in Σ of genus g. If $\dim \langle [\alpha_i]_{i=1}^k \rangle = g$ (in the first homology $H_1(\Sigma; \mathbb{Z}_2)$) then $\boldsymbol{\alpha}$ determines a unique handlebody (unique up to homeomorphism restricting to the identity on the boundary Σ) for which α_i are *compressible*, that is, bound embedded disks in the handlebody. In fact, by attaching 3–dimensional 2–handles to $\Sigma \times [0, 1]$ along the α_i, and then capping off the resulting S^2–boundaries with $(k - g + 1)$ copies of D^3 we recover the handlebody $\mathfrak{U}$ with the above property.

Suppose now that $\alpha_1, \alpha_2, \alpha_1' \subset \Sigma$ are disjoint embedded simple closed curves bounding a pair-of-pants (i.e. a three-punctured sphere) in Σ which is disjoint

from all the other $\boldsymbol{\alpha}$–curves. In this case $\{\alpha_1', \alpha_2\}$ is called the result of the *handleslide* of α_1 over α_2. The significance of this operation follows from

THEOREM 2.2. *The curves* $\boldsymbol{\alpha} = \{\alpha_1, \ldots, \alpha_k\}$ *and* $\boldsymbol{\alpha}' = \{\alpha_1', \ldots, \alpha_k'\}$ *determine the same handlebody if and only if* $\boldsymbol{\alpha}$ *can be transformed to* $\boldsymbol{\alpha}'$ *by a sequence of isotopies and handleslides.*

A *Heegaard diagram* $(\Sigma, \boldsymbol{\alpha}, \boldsymbol{\beta})$ determines a Heegaard decomposition $U_0 \cup_\Sigma U_1$ (by taking U_0 given by $(\Sigma, \boldsymbol{\alpha})$ and U_1 by $(\Sigma, \boldsymbol{\beta})$), and through the Heegaard decomposition therefore $(\Sigma, \boldsymbol{\alpha}, \boldsymbol{\beta})$ determines a 3–manifold $Y = U_0 \cup_\Sigma U_1$. In the following we will always assume that our Heegaard diagrams are *balanced*, that is, $|\boldsymbol{\alpha}| = |\boldsymbol{\beta}|$.

DEFINITION 2.3. Suppose that $(\Sigma, \boldsymbol{\alpha}, \boldsymbol{\beta})$ is a (balanced) Heegaard diagram of Y, where Σ is of genus g and $|\boldsymbol{\alpha}| = k$. Suppose that the set of points $\mathbf{w} = \{w_1, \ldots, w_{k-g+1}\} \subset \Sigma - \boldsymbol{\alpha} - \boldsymbol{\beta}$ satisfies that

  • each component of $\Sigma - \boldsymbol{\alpha}$ contains a unique w_i, and
  • each component of $\Sigma - \boldsymbol{\beta}$ contains a unique w_j.

Then $(\Sigma, \boldsymbol{\alpha}, \boldsymbol{\beta}, \mathbf{w})$ is a *multi-pointed Heegaard diagram* for the 3–manifold Y. The elements of $\mathbf{w}$ are the *basepoints* of the diagram.

EXAMPLES 2.4. • Suppose that α_1 and β_1 are two simple closed curves in S^2 intersecting each other in exactly two points. Let w_1, w_2 be two points in two domains which do not share sides. The result is the (once stabilized) standard spherical Heegaard diagram $\mathfrak{S}_1 = (S^2, \alpha_1, \beta_1, \{w_1, w_2\})$ of S^3.

• Suppose that the torus T^2 is presented as the identification of the top–bottom and left–right sides of a square in the plane. Then n horizontal and n vertical segments in the square close up to n $\boldsymbol{\alpha}$– and n $\boldsymbol{\beta}$–curves, providing a genus-1 Heegaard diagram for the standard toric Heegaard decomposition $\mathfrak{T}$ of the 3–sphere S^3. Placing one w_i in each row in such a manner that also each column has a single w_j, we get a multi-pointed Heegaard diagram $(T^2, \boldsymbol{\alpha}, \boldsymbol{\beta}, \mathbf{w})$ for S^3. For $n = 1$ the resulting Heegaard diagram $(T^2, \alpha_1, \beta_1, w_1)$ will be denoted by $\mathfrak{T}_1$.

• Notice that if we place a further point z_i in each row of the n–pointed toric Heegaard diagram of S^3 in such a manner that each column also contains a unique z_j (only in squares not containing w_i's), we specify a link (multi-component knot) in S^3. Indeed, connect the w_i and the z_j in each column by vertical intervals, and then connect the points w_p and z_q in each row by horizontal intervals. Whenever a vertical and a horizontal segment would meet, apply the convention that the vertical line segment passes over the horizontal one. In this way we get a link L in S^3, with the property that the horizontal intervals are in one handlebody, while the vertical intervals comprising L are in the other handlebody of the standard toric Heegaard decomposition of S^3. The link L intersects the toric Heegaard surface T^2 exactly in the points w_i and z_j. The above presentation of L is called a *grid* presentation, and it is not hard to see that any link in S^3 admits a grid

presentation: consider the modification of an arbitrary projection of L such that the result contains only horizontal and vertical segments, and the vertical segments pass over the horizontal ones.

The following definition (together with the concept of isotopies and handleslides) will play a crucial role in understanding the relation among Heegaard diagrams representing diffeomorphic 3–manifolds.

DEFINITION 2.5. • A *type-g stabilization* of a multi-pointed Heegaard diagram $(\Sigma, \boldsymbol{\alpha}, \boldsymbol{\beta}, \mathbf{w})$ is the connected sum of it with the standard once-pointed toric diagram $\mathfrak{T}_1$ of S^3, where the connected sum is taken in domains containing basepoints (and only one of the two basepoints in the connect-sum domains is kept).
• A *type-b stabilization* of a multi-pointed Heegaard diagram $(\Sigma, \boldsymbol{\alpha}, \boldsymbol{\beta}, \mathbf{w})$ is the connected sum of it with the standard spherical diagram $\mathfrak{S}_1$ of S^3, where the connected sum is taken in domains containing basepoints (and only one of the two basepoints in the connect-sum domains is kept).

With the above definition at hand, we can state the main result of this subsection:

THEOREM 2.6. • *If two Heegaard diagrams differ by isotopy, handleslide or (type-g or type-b) stabilization then the diagrams represent diffeomorphic 3–manifolds.*
• *Suppose that $(\Sigma_i, \boldsymbol{\alpha}_i, \boldsymbol{\beta}_i, \mathbf{w}_i)$ (for $i = 1, 2$) are two multi-pointed Heegaard diagrams of the 3–manifold Y. Then $(\Sigma_1, \boldsymbol{\alpha}_1, \boldsymbol{\beta}_1, \mathbf{w}_1)$ can be transformed into $(\Sigma_2, \boldsymbol{\alpha}_2, \boldsymbol{\beta}_2, \mathbf{w}_2)$ by a finite sequence of isotopies, handleslides and (type-g and type-b) stabilizations and their inverses.*

In the light of this result, a 3–manifold invariant can be defined by constructing an invariant of multi-pointed Heegaard diagrams which does not change under isotopies, handleslides and (type-g and type-b) stabilizations. This is exactly the line of reasoning we will adapt in the next section. Before defining the 3–manifold invarian $\widehat{\mathrm{HF}}_{\mathrm{st}}$, however, we will very briefly review the general concept of Lagrangian Floer homologies.

2.2. Lagrangian Floer homology. Suppose that X^{2n} is a smooth, oriented even–dimensional manifold, and $\omega \in \Omega^2(X)$ is a smooth 2–form which is

- closed, i.e. $d\omega = 0$, and
- nondegenerate, that is, $\omega^n > 0$.

Then the pair (X, ω) is called a *symplectic manifold* and ω a *symplectic form*. A submanifold $L \subset X$ of dimension n with the property that $\omega|_L = 0$ is called a *Lagrangian* submanifold of (X, ω).

Suppose now that we have two Lagrangian submanifolds $L_1, L_2 \subset (X, \omega)$ intersecting each other transversally. In its simplest version (and under the

favourable circumstances indicated in Remarks 2.7), Lagrangian Floer homology associates a chain complex, and hence a homology theory $\mathrm{HF}(L_1, L_2)$ to (X, ω, L_1, L_2). The definition of this chain complex proceeds as follows.

Assume first of all that $L_1 \cap L_2$ is finite, and consider the finite dimensional $\mathbb{Z}_2$ vector space $\mathrm{CF}(L_1, L_2)$ generated by the intersection points $L_1 \cap L_2$. Let J be an almost-complex structure on X, that is, a linear bundle map $J \colon TX \to TX$ satisfying $J^2 = -\mathrm{Id}_{TX}$. Assume furthermore that J is compatible with ω, meaning that $\omega(Jv_1, Jv_2) = \omega(v_1, v_2)$ and $\omega(v, Jv) > 0$ for all $v_1, v_2 \in TX$ and $0 \neq v \in TX$. Let $\mathbb{D}$ denote the unit complex disk $\{z \in \mathbb{C} \mid z\overline{z} \leq 1\}$.

Define the boundary map

$$\partial \colon \mathrm{CF}(L_1 \cap L_2) \to \mathrm{CF}(L_1 \cap L_2)$$

as follows. Fix $\mathbf{x}, \mathbf{y} \in L_1 \cap L_2$ and consider the moduli space $\mathfrak{M}_{\mathbf{xy}}$ of holomorphic maps

$$u \colon \mathbb{D} \to X$$

with the boundary conditions

- $u(\mathrm{i}) = \mathbf{x}$, $u(-\mathrm{i}) = \mathbf{y}$,
- $u(\{z \in \partial\mathbb{D} \mid \mathrm{Re}\, z \geq 0\}) \subset L_1$ and $u(\{z \in \partial\mathbb{D} \mid \mathrm{Re}\, z \leq 0\}) \subset L_2$.

The automorphism group of $\mathbb{D}$ fixing i and $-i$ is isomorphic to $\mathbb{R}$; let the mod 2 number of 0–dimensional components of the factor $\mathfrak{M}_{\mathbf{xy}}/\mathbb{R}$ be denoted by $n_{\mathbf{xy}}$. Then the boundary map is defined as

$$\partial \mathbf{x} = \sum_{\mathbf{y} \in L_1 \cap L_2} n_{\mathbf{xy}} \cdot \mathbf{y}.$$

With ∂ in place, we define the Lagrangian Floer homology of the pair (L_1, L_2) as

$$\mathrm{HF}(L_1, L_2) = H_*(\mathrm{CF}(L_1, L_2), \partial) = \ker \partial / \mathrm{Im}\, \partial.$$

In order the above definitions to make sense, we need specific properties of the symplectic manifold (X, ω) and the Lagrangians L_1, L_2. We will just list these concerns and do not provide sufficient conditions under which these hold.

REMARKS 2.7. (a) In the definition we assumed that the intersection $L_1 \cap L_2$ is finite – this is usually a simple consequence of some compactness assumption we make when applying the above scheme.

(b) To have smooth moduli spaces (with the expected dimensions predicted by the index formula) we need to choose a sufficiently generic almost-complex structure.

(c) In order to have a well-defined value for $n_{\mathbf{xy}}$ we need some assumptions which ensure that there are only finitely many 0–dimensional components of the factor $\mathfrak{M}_{\mathbf{xy}}/\mathbb{R}$.

(d) We need to verify that the square ∂^2 of the boundary operator vanishes, i.e. we get that $\mathrm{Im}\, \partial \leq \ker \partial$. This delicate property of a Lagrangian theory

(which is often not satisfied) ensured that $(\mathrm{CF}(L_1, L_2), \partial)$ is indeed a chain complex, and hence the step of taking the homology does make sense.

(e) Under the appropriate conditions, the resulting homology theory admits the following invariance feature: if L_1 and L_1' are *Hamiltonian isotopic*, then the groups $\mathrm{HF}(L_1, L_2)$ and $\mathrm{HF}(L_1', L_2)$ are isomorphic.

3. HEEGAARD FLOER GROUPS

Suppose that $(\Sigma, \boldsymbol{\alpha}, \boldsymbol{\beta}, \mathbf{w})$ is a multi-punctured Heegaard diagram of the closed, oriented 3–manifold Y. Consider the k–fold symmetric power $\mathrm{Sym}^k(\Sigma)$, i.e. the factor of the k–fold power $\times_1^k \Sigma$ with the natural action of the symmetric group S_k on k letters. Although symmetric powers are typically not manifolds, the symmetric power of a 2–dimensional surface is a smooth manifold. In addition, it also admits a symplectic structure; according to [8] this structure can be chosen to be the factor of a product structure on $\times_1^k \Sigma$ away from the diagonal. The product of the $\boldsymbol{\alpha}$–curves (and similarly of the $\boldsymbol{\beta}$–curves) provides an embedded torus $\mathbb{T}_\alpha$ (and a torus $\mathbb{T}_\beta$) of dimension k. It is straightforward to check that these tori are Lagrangian submanifolds, and since $\boldsymbol{\alpha}$ and $\boldsymbol{\beta}$ intersect transversally, so do the tori $\mathbb{T}_\alpha$ and $\mathbb{T}_\beta$. Before proceeding further in constructing the Heegaard Floer homology groups, we need a few definitions regarding Heegaard diagrams.

DEFINITION 3.1. Suppose that $\mathfrak{D} = (\Sigma, \boldsymbol{\alpha}, \boldsymbol{\beta}, \mathbf{w})$ is a multi-pointed Heegaard diagram of the 3–manifold Y.

• A connected component D_i of $\Sigma - \boldsymbol{\alpha} - \boldsymbol{\beta}$ is called an *elementary domain*. Suppose therefore that $\Sigma - \boldsymbol{\alpha} - \boldsymbol{\beta} = \cup_i D_i$. The formal linear combination $D = \sum n_i D_i$ (with $n_i \in \mathbb{Z}$) of elementary domains is a *domain*. Since an elementary domain is a 2–dimensional submanifold-with-boundary of Σ, each D_i defines a 2–chain, and hence each domain D defines a 2–chain in the Heegaard surface Σ.

• The boundary ∂D is by definition the boundary of this 2–chain.

• Suppose that D is a domain and D_i is an elementary domain. Then the *multiplicity* of D_i in D is simply the coefficient n_i of D_i in the formal linear combination defining D.

• Let $\mathbf{x}$ and $\mathbf{y}$ denote two intesection points of $\mathbb{T}_\alpha$ and $\mathbb{T}_\beta$. The set $\pi_2(\mathbf{x}, \mathbf{y})$ comprises of those domains D for which ∂D has the property that $\partial(\partial D \cap \boldsymbol{\alpha}) = \mathbf{y} - \mathbf{x}$ and $\partial(\partial D \cap \boldsymbol{\beta}) = \mathbf{x} - \mathbf{y}$.

Notice that if u is a holomorphic map from $\mathbb{D}$ to X, then u naturally defines a domain $D(u)$ by taking the multiplicity of the elementary domain D_i to be equal to the intersection number $u(\mathbb{D}) \cap (\{d_i\} \times \mathrm{Sym}^{k-1}(\Sigma))$ for a point $d_i \in D_i$. Since the almost-complex structure J can be chosen in such a way that $\{d_i\} \times \mathrm{Sym}^{k-1}(\Sigma)$ is J–holomorphic for all i, we get that $D(u)$ is nonnegative (i.e. $n_i \geq 0$ for all coefficients in $D(u) = \sum_i n_i D_i$) once u is a holomorphic map. Now we define the concept admissibility.

DEFINITION 3.2. The domain D in the multi-pointed Heegaard diagram $\mathfrak{D}$ is a *periodic domain* if $D \in \pi_2(\mathbf{x}, \mathbf{x}) = \pi_2(\mathbf{x})$ for some $\mathbf{x}$, that is, ∂D is the union of complete $\boldsymbol{\alpha}$– and $\boldsymbol{\beta}$–curves, and for all basepoints w_i we have that the multiplicity of the elementary domain containing w_i is zero in D. The multi-pointed Heegaard diagram $\mathfrak{D}$ is *admissible* if for all nonzero periodic domain P, its defining formal linear combination involves both positive and negative coefficients.

Now the application of the Lagranian Floer homology scheme discussed in Subsection 2.2 for $(\mathrm{Sym}^k(\Sigma), \mathbb{T}_\alpha, \mathbb{T}_\beta)$ (and with the requirement that $u(\mathbb{D}) \cap (\{w_i\} \times \mathrm{Sym}^{k-1}(\Sigma) = \emptyset)$ provides a chain complex $(\widehat{\mathrm{CF}}(\mathfrak{D}), \partial)$ and a homology theory, denoted by $\widehat{\mathrm{HF}}(\mathfrak{D})$. In [7] it has been shown that for admissible an multi-pointed Heegaard diagram the resulting Lagrangian Floer homology is well-defined, and produces the *Heegaard Floer homology group* $\widehat{\mathrm{HF}}(\mathfrak{D})$. In order to state the precise result about the invariance of the resulting group, we need two more definitions.

DEFINITION 3.3. The pairs (V_1, b_1) and (V_2, b_2) of $\mathbb{Z}_2$ vector spaces V_i and positive integers b_i are *equivalent* if (with the assumption $b_1 \geq b_2$) we have that $V_1 = V_2 \otimes (\mathbb{Z}_2 \oplus \mathbb{Z}_2)^{\otimes(b_1 - b_2)}$. The equivalence class of the pair (V, b) will be denoted by $[V, b]$.

DEFINITION 3.4. Suppose that $\mathfrak{D} = (\Sigma, \boldsymbol{\alpha}, \boldsymbol{\beta}, \mathbf{w})$ is an admissible multi-pointed Heegaard diagram of Y. Define $b(\mathfrak{D})$ as the cardinality $|\mathbf{w}|$ of the basepoint set, and take $\widehat{\mathrm{HF}}_{\mathrm{st}}(\mathfrak{D})$ to be equal to $[\widehat{\mathrm{HF}}(\mathfrak{D}), b(\mathfrak{D})]$.

THEOREM 3.5 (Ozsváth–Szabó [7]). *Suppose that $\mathfrak{D} = (\Sigma, \boldsymbol{\alpha}, \boldsymbol{\beta}, \mathbf{w})$ is an admissible multi-pointed Heegaard diagram of the closed, oriented 3–manifold Y. Then the associated Lagrangian Floer homology $\widehat{\mathrm{HF}}(\mathfrak{D})$ is well-defined. For two admissible diagrams $\mathfrak{D}_1$ and $\mathfrak{D}_2$ of Y the resulting homologies $\widehat{\mathrm{HF}}(\mathfrak{D}_1)$ and $\widehat{\mathrm{HF}}(\mathfrak{D}_2)$ satisfy*

$$[\widehat{\mathrm{HF}}(\mathfrak{D}_1), b(\mathfrak{D}_1)] = [\widehat{\mathrm{HF}}(\mathfrak{D}_2), b(\mathfrak{D}_2)],$$

hence the stabil Heegaard Floer homology $\widehat{\mathrm{HF}}_{\mathrm{st}}(Y) = [\widehat{\mathrm{HF}}(\mathfrak{D}), b(\mathfrak{D})]$ of Y (for some admissible diagram $\mathfrak{D}$) is a diffeomorphism invariant of Y.

REMARKS 3.6. • The proof of the theorem relies on the application of Theorem 2.6. The effect of stabilizations can be determined in a fairly simple manner. It has been shown in [8] that both isotopies and handleslides induce Hamiltonian isotopies on the corresponding tori $\mathbb{T}_\alpha$ or $\mathbb{T}_\beta$, hence the generic property of Lagrangian Floer homologies being invariant under Hamiltonian isotopies (cf. Remarks 2.7) implies that the diagrams related by isotopy or handleslide give rise to equal stable Heegaard Floer groups.

• In the original version of the definition of Heegaard Floer homologies (as it is given in [7]) the authors considered only once-punctured diagrams, resulting the groups $\widehat{\mathrm{HF}}$ without the stable property. Also, the groups were

equipped with many extra structures (a spin^c grading, and a homological grading), and further variants of the groups were defined (which are modules over polynomial rings rather than $\mathbb{Z}_2$ vector spaces). These constructions led to 4–manifold invariants and provided the basis of many striking new results in low dimensional topology. In the present note we chose to discuss the stable hat-version because of its simplicity and computability.

4. NICE DIAGRAMS

The computation of the boundary map ∂ is rather complicated in general. It was the crucial observation of Sarkar and Wang that for specific Heegaard diagrams ∂ can be computed in a fairly simple combinatorial way.

DEFINITION 4.1. Suppose that $\mathfrak{D}$ is a multi-pointed Heegaard diagram of Y.

• An elementary domain D_i is a $2n$–gon if D_i is simply connected and has $2n$ intersection points on its boundary ∂D_i. For $n = 1$ we say that D_i is a *bigon*, for $n = 2$ it is a *rectangle*.

• We say that $\mathfrak{D}$ is *nice* if for every elementary domain D_i in the diagram either D_i contains a basepoint, or D_i is a bigon, or D_i is a rectangle.

DEFINITION 4.2. Fix a multi-pointed Heegaard diagram $\mathfrak{D}$, and consider two intersection points $\mathbf{x}$ and $\mathbf{y}$. A domain $D \in \pi_2(\mathbf{x}, \mathbf{y})$ is an *embedded $2n$–gon* if

- in the formal linear combination $D = \sum n_i D_i$ all coefficients are either 0 or 1,
- the union of the closures of D_i with $n_i = 1$ is a simply connected subspace of Σ, having exactly $2n$ intersection points on its boundary, and
- at each intersection point on ∂D exactly one of the four quandrants meeting at that point have multiplicity 1 and all the others have multiplicity 0.

As before, for $n = 1$ the $2n$–gon is also called a *bigon*, while for $n = 2$ it is a *rectangle*. The $2n$–gon is *empty* if none of the D_i with $n_i = 1$ contain basepoints, and at any coordinate x_i of $\mathbf{x}$ (and y_j of $\mathbf{y}$) at most one of the quadrant meeting at x_i (or y_j) has multiplicity 1.

The following simple property of a nice diagram will turn out to be very useful later.

LEMMA 4.3. *Suppose that $\mathfrak{D}$ is a nice diagram. If α_i is an $\boldsymbol{\alpha}$–curve in the diagram, then on either side of this curve there is an elementary domain containing a basepoint.*

Proof. In fact, if on one side there is no such elementary domain, then either all elementary domains on this side of α_i are rectangles (which implies that there is a parallel $\boldsymbol{\alpha}$–curve α_j determining an annullar component with

no basepoint), or there are two bigons and some rectangles, in which case α_i is the boundary of a disk-component of $\Sigma - \boldsymbol{\alpha}$ having no basepoint. Since every component in a multi-punctured Heegaard diagram contains a (unique) basepoint, we reached a contradiction. $\square$

LEMMA 4.4. *A nice diagram is admissible.*

Proof. For a periodic domain P we need that ∂P is a union of complete $\boldsymbol{\alpha}$– and $\boldsymbol{\beta}$–curves. Since next to every curve in the boundary there is a basepoint, and there the multiplicity of P is zero, we get that $P = 0$, concluding the proof. $\square$

Recall that in the definition of the Heegaard Floer groups an almost-complex structure J must be fixed, and then we can consider the moduli space of holomorphic maps with the prescribed boundary values. The number of such holomorphic representatives typically depends on the chosen almost-complex structure. In a nice diagram, however, there is no such dependence. (The reason is that in nice diagrams – because of purely topological reasons – there are no Maslov index 0, nonnegative domains.) The following result of Sarkar and Wang provides a combinatorial description of ∂ in nice diagrams.

THEOREM 4.5 (Sarkar–Wang [10]). *Suppose that $\mathfrak{D}$ is a nice diagram, and $\mathbf{x}, \mathbf{y} \in \mathbb{T}_\alpha \cap \mathbb{T}_\beta$ are two intersection points. Then $n_{\mathbf{xy}}$ defined using the factor of the moduli space of holomorphic disks connecting $\mathbf{x}$ and $\mathbf{y}$ is equal (mod 2) to the number of empty embedded bigons and rectangles connecting $\mathbf{x}$ and $\mathbf{y}$ in the diagram.*

REMARK 4.6. The proof of the above theorem relies on the fact that using a nice diagram any holomorphic map encountered in the definition of ∂ gives rise to an empty bigon or rectangle, and conversely, an empty bigon or rectangle admits a unique holomorphic representative in $\mathfrak{M}_{\mathbf{xy}}/\mathbb{R}$. All the finiteness concerns listed in Remark 2.7 are automatically taken care of in a nice diagram. For example, the proof of $\partial^2 = 0$ is an exercise resting on some simple planar geometry, cf. [6].

The above theorem shows that having a nice diagram for a 3–manifold Y makes the computation of the Heegaard Floer groups particularly convenient. At this point, however, it is unclear, what class of 3–manifolds admit nice Heegaard diagrams. According to a result of Sarkar and Wang [10], in fact, having such a diagram is not a restriction on the 3–manifold:

THEOREM 4.7 (Sarkar-Wang [10]). *Any 3–manifold Y admits a nice Heegaard diagram. In fact, if $(\Sigma, \boldsymbol{\alpha}, \boldsymbol{\beta}, w)$ is a once-punctured Heegaard diagram of Y, then an appropriate sequence of isotopies and handleslides of the $\boldsymbol{\beta}$–curves turn it into nice.*

In the next section we will show a recipe for finding a nice (multi-pointed) Heegaard diagram of a 3–manifold Y based on the branched cover construction, and also show how to get a simple description of the Heegaard Floer chain complex from such a presentation.

5. ADAPTED DIAGRAMS

A smooth map $f\colon X_1 \to X_2$ between the n–manifolds X_1, X_2 is a d–*fold branched cover* if there is a codimension–2 submanifold N in X_2 such that over the complement $X_2 - N$ the map f is an ordinary d–fold covering map. If N is minimal with this property, then it can be presented as $f(B) = N$, the image of the *singular set B* where f is not (locally) injective. The d–fold cover over $X_2 - N$ can be given by the monodromy representation, which is a homomorphism (defined up to conjugacy)

$$p\colon \pi_1(X_2 - N) \to S_d,$$

where S_d is the symmetric group on d letters. The image of p on the meridians of N determine the structure of the cover; if all meridians are mapped to transpositions, the branched cover is called *simple*. In the following we will only consider double and simple triple branched covers. Double branched covers are much easier to handle from our point of view, so we start our discussion with such covers. On the other hand, not every 3–manifold admits a double branched cover presentation along a link in S^3. According to a famous result of Hilden and Montesinos [3, 4] every 3–manifold can be presented as a simple triple branched cover of S^3. We will therefore extend the constructions found for the double branched covers to the case of simple triple branched covers.

5.1. Double branched covers. For an alternate description of the double branched cover construction, let $N \subset X_2$ be a codimension-2 submanifold, and let $\mathcal{L} \to X_2$ denote the line bundle with $c_1(\mathcal{L}) = PD([N]) \in H^2(X_2; \mathbb{Z})$. If $c_1(\mathcal{L})$ is divisible by 2 in $H^2(X_2; \mathbb{Z})$, and $2a = c_1(\mathcal{L})$ then for the line bundle $\mathcal{K}$ with $c_1(\mathcal{K}) = a$ we have $\mathcal{K} \otimes \mathcal{K} = \mathcal{L}$. Take a section σ of $\mathcal{L}$ with $\sigma^{-1}(0) = N$ and let $X_1 = \{q_x \in \mathcal{K} \mid q_x \otimes q_x = \sigma(x)\}$ for all $x \in X_2$. The restriction of the bundle map to $X_1 \subset \mathcal{K}$ then provides a double branched cover $f\colon X_1 \to X_2$ branched along N. Notice that the construction depends on the choice of $a \in H^2(X_2; \mathbb{Z})$ satisfying $2a = c_1(\mathcal{L})$. For $X_2 = S^3$ there is no 2–torsion in the second cohomology (in fact, that group is trivial), hence the double branched cover of S^3 along a link is unique. (If $PD([N])$ is not divisible by two in $H^2(X_2; \mathbb{Z})$, there is no double branched cover of X_2 with branched set N.)

So consider a link $L \subset S^3$, and take Y to be the double branched cover of S^3 branched along L. Since the meridians generate $\pi_1(S^3 - L)$, and they are all mapped to the single nontrivial element of $S_2 = \mathbb{Z}_2$, the 3–manifold Y is determined by L. In the following we will produce a nice Heegaard diagram for Y and compute the Heegaard Floer homology of Y using that particular

diagram. To this end, put the branch set L in a grid diagram, as it is discussed in Examples 2.4. Suppose that the result is an $n \times n$ grid. For every annular region between two neighbouring $\boldsymbol{\alpha}$–curve α_i and α_{i+1} put a new curve $\alpha_{i+\frac{1}{2}}$, which is parallel to the boundaries but separates the two points z_i and w_j. (These will be the *new* curves, the other ones are the *old* curves.) Add the similar $\boldsymbol{\beta}$–curves. The grid together with the new curves will be referred to as the *extended grid*. When starting with an $n \times n$ grid, the result will be of dimension $2n \times 2n$.

THEOREM 5.1. *The pull-back of the extended grid diagram provides a Heegaard diagram $\mathfrak{D}$ for Y which has only octagons and rectangles as elementary domains. By placing a basepoint in each octagon, we get a nice Heegaard diagram for Y.*

Proof. The addition of the new curves turns the grid presentation of L into a multi-pointed toric Heegaard diagram of S^3, since the baspoints which previously shared a component now became separated. Denote the toric Heegaard diagram of S^3 defined by the extended grid by $\mathfrak{T}_{grid}$. It is easy to see that the double branched cover of the solid torus along the n arcs of L falling into this handlebody is a handlebody of genus $n + 1$. The old $\boldsymbol{\alpha}$–curves in the grid bound disks disjoint from the branch link L, therefore an old curve lifts to two disjoint copies of circles in the 3–manifold, both bounding disk in the appropriate handlebody. A new curve bounds a disk in S^3 which intersects the branch locus in a single point, hence a new curve lifts to a single component, still bounding a disk in the handlebody (since the double branched cover of a disk branched in a point is a disk again).

In conclusion, with considering the pull-back we get $3n$ disjoint $\boldsymbol{\alpha}$– (and similarly $3n$ disjoint $\boldsymbol{\beta}$–) curves in the genus-$(n+1)$ surface, providing a Heegaard diagram $\mathfrak{D}$ of Y. The components of $T^2 - \boldsymbol{\alpha}$ in the extended grid are all annuli, containing unique basepoints. Their inverse images are all pair-of-pants, hence the $3n$ $\boldsymbol{\alpha}$–curves (and similarly the $3n$ $\boldsymbol{\beta}$–curves) provide a pair-of-pants decomposition of the Heegaard surface Σ of the diagram $\mathfrak{D}$. Notice that since the f–image of any of the $\boldsymbol{\alpha}$–curves in $\mathfrak{D}$ is homologically essential in the torus, all $\boldsymbol{\alpha}$–curves (and similarly all $\boldsymbol{\beta}$–curves) in $\mathfrak{D}$ are homologically essential. An elementary domain in $\mathfrak{D}$ is clearly the inverse image of an elementary domain of the toric diagram $\mathfrak{T}_{grid}$. Therefore an elementary domain D_i of $\mathfrak{D}$ either covers a rectangle of $\mathfrak{T}_{grid}$ which contains no basepoint, in which case D_i is also a rectangle, or it covers an elementary domain with a basepoint, in which case D_i is an octagon. Since each pair-of-pants component contains a unique octagon, by placing the basepoints into them, we get a nice diagram. $\qquad\square$

DEFINITION 5.2. A Heegaard diagram of Y given by the aid of a double branched cover as above is called an *adapted* diagram.

Next we would like to understand the intersection points and the empty rectangles of the adapted diagram $\mathfrak{D}$ when working only in the extended grid

downstairs. To this end, fix a point P in the torus, which is an intersection of an old $\boldsymbol{\alpha}$– and an old $\boldsymbol{\beta}$–curve α_1 and β_1 in $\mathfrak{T}_{grid}$. Cut the torus open along these curves and get a square in the plane. Connect the two branch points in an annular old $\boldsymbol{\alpha}$–component with an arc ℓ_b which is disjoint from the chosen β_1. (We assume that these line segments ℓ_b avoid all intersection points.) Recall that over every point of the torus (except the basepoints $\mathbf{z}$ and $\mathbf{w}$) there are two points of the Heegaard surface $\Sigma \subset Y$. We chose the arcs ℓ_b to handle the two sheets of the double cover away from $\mathbf{z}$ and $\mathbf{w}$: consider a point $u \in T^2 - \mathbf{z} - \mathbf{w}$ and choose one of its inverse images in Σ. By lifting a path from u to any other $v \in T^2 - \mathbf{z} - \mathbf{w}$ avoiding $\cup_b \ell_b$ we uniquely determine one of the two points of Σ which map to v. For another path with the same property the result will be the same, since a closed loop in $T^2 - \alpha_1 - \beta_1 - \cup_b \ell_b$ encircles an even number of branch points, and hence the lift of a closed loop in $T^2 - \alpha_1 - \beta_1 - \cup_b \ell_b$ is a closed loop in Σ. This convention will help us handling the relation for points of Σ to be on the same sheet. Indeed, by fixing one point of Σ (out of the two) over $P = \alpha_1 \cap \beta_1$, we can select one inverse image for any intersection point x in the grid: connect P with x in $T^2 - \alpha_1 - \beta_1 - \cup_b \ell_b$ and lift this path starting at the chosen point over P; the endpoint will be independent of the chosen path, and provides an equivalence class of points of Σ which we regard to be one of the sheets. With these preparations, now we are ready to identify the generators and the differential of $(\widehat{\mathrm{CF}}(\mathfrak{D}), \partial)$ down in the extended grid.
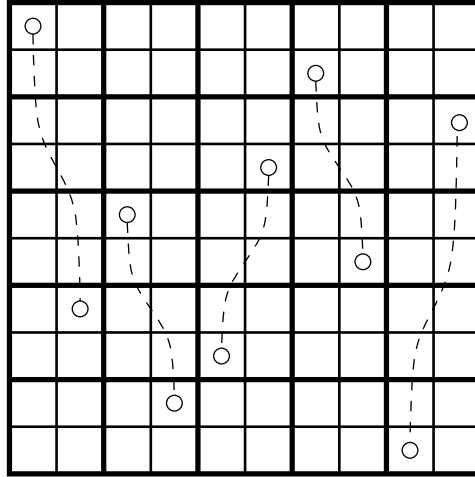
P

Fig. 5.1 – An example of an extended grid diagram. The heavy lines correspond to old $\boldsymbol{\alpha}$– and $\boldsymbol{\beta}$–curves, while the lighter ones are the new curves. The branch points are symbolized by circles, and the dashed lines show the arcs ℓ_b connecting the basepoints. The lower left corner is P, the lines passing through it are the chosen curves α_1 and β_1.

The generators. Associate two symbols $q^{\pm}$ to every intersection point q (of the $\boldsymbol{\alpha}$– and $\boldsymbol{\beta}$–curves) in the extended grid. For two points q, q' which are either in the same vertical or in the same horizontal line, define $v_{qq'}$ as the intersection number of the joining line segment with $\cup_b \ell_b$.

DEFINITION 5.3. We define the *set G of generators* as the set of unordered $3n$–tuples $\mathbf{x} = \{x_1^{\epsilon_1}, \ldots, x_{3n}^{\epsilon_{3n}}\}$ of intersection points as follows

(1) for all i the symbol x_i stands for an intersection point in the extended grid and $\epsilon_i \in \{\pm 1\}$ is a sign;

(2) every new $\boldsymbol{\alpha}$– and $\boldsymbol{\beta}$–curve in the extended grid admits a unique coordinate of $\mathbf{x}$;

(3) every old $\boldsymbol{\alpha}$– and $\boldsymbol{\beta}$–curve in the extended grid admits exactly two coordinate of $\mathbf{x}$;

(4) if $x_i^{\epsilon_i}$ and $x_j^{\epsilon_j}$ are two coordinates of $\mathbf{x}$ on the same old α–curve then $\epsilon_i \cdot \epsilon_j = -(-1)^{v_{x_i x_j}}$, and

(5) if $x_i^{\epsilon_i}$ and $x_j^{\epsilon_j}$ are two coordinates of $\mathbf{x}$ on the same old β–curve then $\epsilon_i \cdot \epsilon_j = -(-1)^{v_{x_i x_j}}$

REMARK 5.4. The requirements in (4) and (5) ensure that the two points $x_i^{\epsilon_i}$ and $x_j^{\epsilon_j}$ are on two distinct components of the inverse image of an old curve.

PROPOSITION 5.5. *The set of intersection points $\mathbb{T}_\alpha \cap \mathbb{T}_\beta$ of the adapted diagram $\mathfrak{D}$ for Y is in 1-1 correspondence with the set G of generators defined above.*

Proof. Indeed, consider an element $\mathbf{x} \in \mathbb{T}_\alpha \cap \mathbb{T}_\beta$. By definition, $\mathbf{x}$ has a coordinate from each $\boldsymbol{\alpha}$– and each $\boldsymbol{\beta}$–curve in $\mathfrak{D}$. Consider the image of the coordinates of $\mathbf{x}$ under the branched cover map f (and still denote the resulting $f(\mathbf{x})$ by $\mathbf{x}$). Since the inverse image of a new curve is connected, we get a single coordinate on each new curve. Since the inverse image of an old curve has two components in $\mathfrak{D}$, we get two coordinates on each old curve. As it is pointed out above, conditions (4) and (5) of Definition 5.3 exactly describe the fact that the two coordinates are on different components of the inverse image of the old curve. $\square$

Therefore the generators described above serve as generators of the Heegaard Floer chain complex $\widehat{\mathrm{CF}}(\mathfrak{D})$.

The differential. Suppose that $\mathbf{x} \in G$ is a generator. Next we define a differential ∂' as

$$\partial' \mathbf{x} = \sum_{\mathbf{y} \in G} r(\mathbf{x}, \mathbf{y}) \cdot \mathbf{y},$$

where $r(\mathbf{x}, \mathbf{y}) = |Rect^o(\mathbf{x}, \mathbf{y})| \bmod 2$, and $Rect^o(\mathbf{x}, \mathbf{y})$ denotes the set of *empty rectangles* connecting $\mathbf{x}$ and $\mathbf{y}$, and whose definition will be given presently.

First we define $Rect(\mathbf{x}, \mathbf{y})$ (the set of rectangles connecting $\mathbf{x}$ and $\mathbf{y}$), and $Rect^o(\mathbf{x}, \mathbf{y})$ will be a subset of $Rect(\mathbf{x}, \mathbf{y})$.

First of all, $Rect(\mathbf{x}, \mathbf{y}) = \emptyset$ unless $\mathbf{x}$ and $\mathbf{y}$ differ exactly at two coordinates. Suppose now that $\mathbf{x}$ and $\mathbf{y}$ differ at the ith and j^{th} coordinate, where the coordinates are $(x_i^{\epsilon_i}, x_j^{\epsilon_j})$ and $(y_i^{\epsilon_i'}, y_j^{\epsilon_j'})$, resp. If the corresponding four points (x_i, y_i, x_j, y_j) are not all distinct, then we define $Rect(\mathbf{x}, \mathbf{y}) = \emptyset$. If the four points (x_i, y_i, x_j, y_j) are all distinct, then they determine two rectangles R_1 and R_2 in the extended grid diagram: consider those rectangles in the torus which have these four points as vertices (there are four such on the torus), and select those two for which the surface orientation induces the orientation on the horizontal ($\boldsymbol{\alpha}$–) arcs the direction from the $\mathbf{x}$–coordinate to the $\mathbf{y}$–coordinate.

For the various cases we discuss whether the rectangle is in $Rect(\mathbf{x}, \mathbf{y})$ and whether it is empty in a case-by-case basis. In case (A) (shown by Figure 5.2)
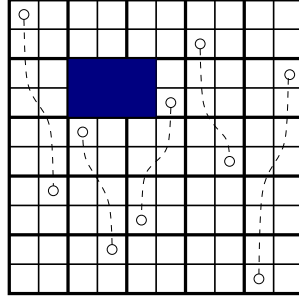

Fig. 5.2 – Various squares in the extended grid diagram: case (A).

we require

CONDITION 5.6. (1) $\epsilon_i = (-1)^{v_{x_i y_i}} \epsilon_i'$, $\epsilon_j = (-1)^{v_{x_j y_j}} \epsilon_j'$, $\epsilon_i = (-1)^{v_{x_i y_j}} \epsilon_j'$ and $\epsilon_j = (-1)^{v_{y_i x_j}} \epsilon_i'$ and

(2) the rectangle is *empty*, that is, it does not contain any branch point z_i or w_j and a further property is satisfied: the line segments ℓ_b partition the rectangle into smaller domains, and each gets a sign by an alternating fashion, where the domains containing points among the vertices x_i, x_j, y_i, y_j have the sign ϵ of the vertex. If there is a further coordinate k with $x_k = y_k$ in the rectangle, then for $r \in Rect^o(\mathbf{x}, \mathbf{y})$ we require the exponent ϵ_k of x_k to have the opposite sign of the smaller domain it sits in.

(These requirements imply that (i) the rectangle in the grid is the projection of a rectangle in $\Sigma \subset Y$ and (ii) in Σ the corresponding rectangle does not contain a basepoint or further coordinates of $\mathbf{x}$ and $\mathbf{y}$, that is, it is empty.) This finishes the list of properties we require from r to be in $Rect^o(\mathbf{x}, \mathbf{y})$ in case (A).

For case (B) (given by Figure 5.3) the conditions are changed a little bit: For the horizontal segments we keep the old conditions (i.e., for relations between
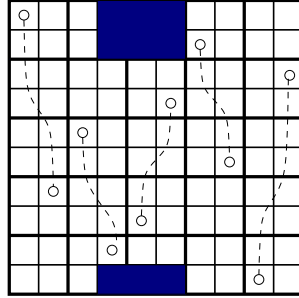
Fig. 5.3 – Various squares in the extended grid diagram: case (B).

signs of x_i, y_j, and between y_i, x_j). For the vertical ones, however, we need to modify the condition slightly: if x_i and y_i are on an old $\boldsymbol{\alpha}$–curve then the condition is the same as before, while in case these points are on a new $\boldsymbol{\alpha}$–curve, the relation is replaced by its opposite: $\epsilon_i = -(-1)^{v_{x_i y_i}} \epsilon_i'$. The exact same modification applies for the pair y_j, x_j. For case (C) (of Figure 5.4) we change the roles of horizontal and vertical in the above modification, and finally for case (D) (as shown by Figure 5.5) we apply the modification for both the horizontal and vertical segments.
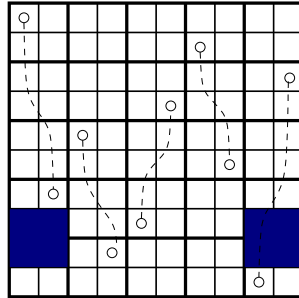

Fig. 5.4 – Various squares in the extended grid diagram: case (C).

With this definition at hand, since the set G of generators has been identified with $\mathbb{T}_\alpha \cap \mathbb{T}_\beta$, we get a map

$$\partial' : \widehat{\mathrm{CF}}(\mathfrak{D}) \to \widehat{\mathrm{CF}}(\mathfrak{D}).$$

The content of the next proposition is that this is exactly the differential definining the Heegaard Floer groups.

PROPOSITION 5.7. *The map ∂' defined above using only the combinatorics of the extended grid is equal to the boundary map ∂ of the chain complex defininig the Heegaard Floer homology group $\widehat{\mathrm{HF}}(\mathfrak{D})$.*
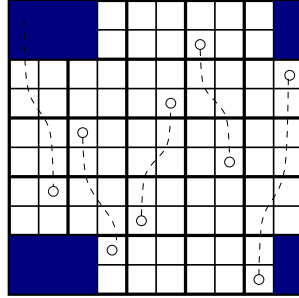
Fig. 5.5 – Various squares in the extended grid diagram: case (D).

Proof. Recall that the boundary map ∂ (although it is defined using holomorphic geometry) can be computed by counting the empty bigons and rectangles connecting intersection points in $\mathfrak{D}$. Since $\mathfrak{D}$ contains only rectangles and octagons (and all octagons admit basepoints), we need to identify the empty rectangles of $\mathfrak{D}$ connecting generators with objects down in the extended grid.

We only need to show that an empty rectangle in $\mathfrak{D}$ projects injectively to an element encountered above in the extended grid. The fact that all such projections are considered by the above description is rather simple.

Suppose therefore that D is an empty rectangle in $\mathfrak{D}$ with four corner points P_1, P_2, P_3, P_4. The map f is obviously injective on the sides of the rectangle: suppose f is not injective on the side connecting, say, P_1 and P_2, and assume first that P_1 is connected to P_2 on an old curve. Since f is a bijection between one of the old curves in Y mapping to the old curve in the toric diagram of S^3, this means that when passing from P_1 to P_2 we use the entire old curve. On the other hand, any curve contains a basepoint on its either side (cf. Lemma 4.3), hence the noninjectivity contradicts the emptyness of D. Similarly, if f is not injective on the side connecting P_1 and P_2 on a new curve, then it must pass by an octagon on each side, having a basepoint in it, contradicting emptyness again. This final argument completes the proof. $\square$

5.2. Triple branched covers. It is a classic result in 3–dimensional topology that any closed oriented 3–manifold Y can be presented as a simple 3–fold branched cover of S^3 [3, 4]. The manifold Y can be recovered from the branch set L (which is a link in S^3), together with the representation $p\colon \pi_1(S^3 - L) \to S_3$ defininig the triple cover over the complement of L. Since $\pi_1(S^3 - L)$ is generated by the meridians of L, and in a simple branched cover meridians are mapped into transposition, we only need to record these images. Consider a projection of L and imagine the basepoint of the fundamental group $\pi_1(S^3 - L)$ of the complement is high over this plane; then along an arc of the projection the meridian is constant, and the image of this meridian can be coded by coloring the arc (by choosing, say (12) to be red, (23) to be white and (13) to be green). (The result will be a three-colored projection of the link L.)

Therefore the branched cover can be coded by a three-colored link projection, which we can assume to be in a grid. So as before, consider a grid presentation of L, that is, a genus-1 Heegaard decomposition of S^3 with n parallel $\boldsymbol{\alpha}$– and $\boldsymbol{\beta}$–curves and with w_i's and z_j's describing the link L. The branched cover then naturally defines a Heegaard decomposition of Y by pulling back the decomposition of S^3, and the inverses of the $\boldsymbol{\alpha}$– and $\boldsymbol{\beta}$–curves lift to a Heegaard diagram of Y. Let the inverse image of the Heegaard torus of S^3 be denoted by $\Sigma \subset Y$. Since Σ is a simple 3–fold branched cover of the torus in $2n$ points, its genus can be easily computed to be equal to $n + 1$. Since an $\boldsymbol{\alpha}$–curve in the torus $\subset S^3$ bounds a disk in the corresponding handlebody, it lifts to three disjoint copies in Σ (and similarly with the $\boldsymbol{\beta}$–curves). An annular region $A_{i,i+1}$ between two neighbouring $\boldsymbol{\alpha}$–curves α_i and α_{i+1} in the grid diagram (containing two branch points) lifts to a two–component surface: one of the components is an annulus and the other is a 4–punctured sphere. As we did in the case of double branched cover, for every such annular $\boldsymbol{\alpha}$–region in the grid we introduce a new $\boldsymbol{\alpha}$–curve $\alpha_{i+\frac{1}{2}}$ in the torus, which is parallel to the two boundary $\boldsymbol{\alpha}$–curves of the annulus, but separates the two branch points. It follows then that the inverse image of this new curve in Σ has two components, one of these components is in the annular component of $f^{-1}(A_{i,i+1})$, while the other one (which double covers the newly chosen $\boldsymbol{\alpha}$–curve $\alpha_{i+\frac{1}{2}}$) is in the 4–punctured sphere component. As before, this $\boldsymbol{\alpha}$–curve separates the 4–punctured sphere into two pairs-of-pants.

Consider now the grid diagram for L together with these newly chosen half–indexed $\boldsymbol{\alpha}$– and $\boldsymbol{\beta}$–curves, i.e., take the extended grid as before. Notice that both the $\boldsymbol{\alpha}$– and the $\boldsymbol{\beta}$–curves partition the torus into $2n$ annuli, each annulus containing a single branch point, resulting in a $2n$–pointed Heegaard diagram for S^3. Every domain in this diagram is a rectangle. Consequently in the branched cover every domain is either a rectangle or an octagon: over a rectangle $\subset T^2 \subset S^3$ with no basepoint we have three rectangles of $\mathfrak{D}$ representing Y, while over a rectangle $\subset T^2 \subset S^3$ containing a basepoint the Heegaard diagram $\mathfrak{D}$ has a rectangle and an octagon. Notice that by putting the basepoints into the octagons in Σ, this time we do not get a multi-pointed Heegaard diagram, since not every component of the complement of the $\boldsymbol{\alpha}$– (or $\boldsymbol{\beta}$–) curves in $\mathfrak{D}$ (representing Y) will admit a basepoint in this way: the annular components do not contain octagons, hence do not contain basepoints either. To fix this problem, either we put in more basepoints, or we delete some of the $\boldsymbol{\alpha}$– (and symmetrically the $\boldsymbol{\beta}$–) curves. We choose to do this latter, by applying the following two conventions: (a) for the new $\boldsymbol{\alpha}$–curves we only consider one component of the inverse image of $\alpha_{i+\frac{1}{2}}$ in Σ, namely the one which double covers the curve downstairs; (b) for the old $\boldsymbol{\alpha}$–curves we only keep the two components of the inverse image of the right endcircle of the annulus which are in the 4–punctured sphere, and do not consider the one in the annular component. To do this step in a coherent way, we fix a

starting old $\boldsymbol{\alpha}$– and $\boldsymbol{\beta}$–circle α_1 and β_1 as before, and orient both. Using the orientation, then every annular region has a rightmost end, and the choice described above can be done coherently.

In conclusion, we get a multi-pointed Heegaard diagram of Y with the properties that

- every domain in the decomposition is either a rectangle or an octagon, and each octagon contains a basepoint; in particular, the decomposition is nice.
- the $\boldsymbol{\alpha}$– and $\boldsymbol{\beta}$–curves both give a pair-of-pants decomposition of Σ;
- each pair-of-pants contains a unique octagon and a number of rectangles;
- an $\boldsymbol{\alpha}$– and a $\boldsymbol{\beta}$–curve either meets exactly once (in case at least one of them is an old curve), or exactly twice (that can happen only if both are new curves).

Notice that over an intersection point of α_i and β_j in the torus there are either two or one intersection points in $\mathfrak{D}$, depending on the choice of the deleted curves. We also lose the property that elementary domains in $\mathfrak{D}$ map to elementary domains down in the extended grid.

The three-coloring of the link L (which we disregarded up to this point) induces a three–coloring of the annuli of the grid as follows. First disregard the new curves. (Recall that we follow the convention that vertical lines pass over horizontals in the link.) In a vertical annulus of the grid the line segment of the link has the same color, let this color be associated to the annulus, and to its right end circle.

The coloring of the horizontal annuli (determined by the old curves) is a little more involved. We say that a conjugate of a color c_1 by another color c_2 is c_1 if $c_1 = c_2$, and is the third color c_3 if $c_1 \neq c_2$. (This rule is modeled on the conjugation rule of transpositions in the symmetric group S_3 on three letters.) Now consider a row in the grid (after the torus has been cut open along the chosen α_1 and β_1 and is considered as a square in the plane), and take the color of a horizontal segment of L in this annulus. Then move to the left end of the row (the annulus became after we cut it open along α_1 and β_1), and whenever we cross a vertical segment of L, conjugate our color with the color of this vertical segment. The resulting color will be the color of the row. Now define the color of an old curve to be the color of the annulus left to it (below it for the horizontal case), and for a new curve the color of it is the color of the annulus containing it. Similarly, the color of a dashed cutting arc ℓ_b is the color of its endpoint (or equivalently, the color of the column it lies in).

Now take an intersection point x of an $\boldsymbol{\alpha}$– and a $\boldsymbol{\beta}$–curves α_i and β_j in the extended grid. The triple branch cover provides three points of Σ over x, but since we deleted some of the $\boldsymbol{\alpha}$– and $\boldsymbol{\beta}$–curves in the diagram upstairs, not all three inverse images of x are intersection points in $\mathfrak{D}$. In fact, the

color-convention is chosen so, that if the colors of α_i and β_j are the same, then there are two intersection points over x, and if the two colors are different then there is a unique intersection point upstairs.

The generators. Next we identify the set of intersection points of $\mathfrak{D}$ down in the extended grid. For any intersection point x of the curves α_i and β_j of colors c_1 and c_2 in the extended grid designate either

- two point when $c_1 = c_2$, and the colors of the two points are the remainig two colors c and c', in notation x^c and $x^{c'}$; or
- one point if $c_1 \neq c_2$, in which case the color of this point is the third color, in notation x^{c_3}.

For the intersection points $x_i, x_j \in T^2$ on the same $\boldsymbol{\alpha}$– (or $\boldsymbol{\beta}$–) curves let $I_{x_i x_j}$ denote the oriented interval joining x_i with x_j on the grid. We define the *set G of generators* as the set of unordered $3n$–tuples $\mathbf{x} = \{x_1^{c_1}, \ldots, x_{3n}^{c_{3n}}\}$ of intersection points as follows

- for all i the symbol x_i stands for an intersection point in the extended grid and $c_i \in \{R, W, G\}$ is a color, which is allowed at that particular intersection point;
- every new $\boldsymbol{\alpha}$– and $\boldsymbol{\beta}$–curve in the extended grid admits a unique coordinate of $\mathbf{x}$;
- every old $\boldsymbol{\alpha}$– and $\boldsymbol{\beta}$–curve in the extended grid admits exactly two coordinates of $\mathbf{x}$;
- if $x_i^{c_i}$ and $x_j^{c_j}$ are two coordinates of $\mathbf{x}$ on the same old $\boldsymbol{\alpha}$– or $\boldsymbol{\beta}$–curve then c_i is distinct from the result of conjugating c_j with all the colors of the dashed lines ℓ_b intersecting the interval $I_{x_j x_i}$.

LEMMA 5.8. *Consider the adapted diagram $\mathfrak{D}$ of Y corresponding to the triple branched cover $f : Y \to S^3$ as above. Then the intersection points $\mathbb{T}_\alpha \cap \mathbb{T}_\beta$ are in 1-1 correspondence with the elements of G.*

Proof. As in the case of double branched covers, the additional requirements above ensure that points with projection on the same old curve are in different inverse images. $\square$

Similarly to the double branched cover case, the differential can be also described in terms of the extended grid (we leave to work out the details to the reader). We note finally that if the 3–manifold Y is given by a surgery presentation then in [1] there is a simple algorithm which determines the three–colored link along which the branched cover construction (with the coloring coding the representation of the fundamental group of the complement) provides Y.

REFERENCES

[1] BOBTCHEVA, I. and PIERGALLINI, R., *Covering moves and Kirby calculus*, arXiv:math/0407032.
[2] GROMOV, M., *Pseudoholomorphic curves in symplectic manifolds*, Invent. Math., **82** (1985), 307–347.

[3] HILDEN, H., *Every closed orientable 3-manifold is a 3-fold branched covering space of S^3*, Bull. Amer. Math. Soc., **80** (1974), 1243–1244.

[4] MONTESINOS, J., *A representation of closed orientable 3-manifolds as 3-fold branched coverings of S^3*, Bull. Amer. Math. Soc., **80** (1974), 845–846.

[5] OZSVÁTH, P., STIPSICZ, A., and SZABÓ, Z., *A combinatorial description of the $U^2 = 0$ version of Heegaard Floer homology*, IMRN, to appear, arXiv:0811.3395.

[6] OZSVÁTH, P., STIPSICZ, A., and SZABÓ, Z., *Combinatorial Heegaard Floer homology and nice Heegaard diagrams*, in preparation, 2009.

[7] OZSVÁTH, P. and SZABÓ, Z., *Holomorphic disks and topological invariants for closed three-manifolds*, Ann. of Math., **159** (2004) 1027–1158.

[8] PERUTZ, T., *Hamiltonian handleslides for Heegaard Floer homology*, Proceedings of Gökova Geometry-Topology Conference 2007, pp. 15–35. GGT Gökova 2008.

[9] REIDEMEISTER, K., *Zur dreidimensionalen Topologie*, Abh. Math. Semin. Hamb. Univ., **9** (1933), 189–194.

[10] SARKAR, S. and WANG, J., *An algorithm for computing some Heegaard Floer homologies*, arXiv:math/0607777.

[11] SINGER, J., *Three-dimensional manifolds and their Heegaard diagrams*, Trans. Amer. Math. Soc., **35** (1933), 88–111.

Hungarian Academy of Sciences
Rényi Institute of Mathematics
Reáltanoda utca 13–15
Budapest, Hungary
E-mail: `stipsicz@math-inst.hu`